STUDY ON TIME-OF-FLIGHT ESTIMATION IN ULTRASONIC WELL LOGGING TOOL: MODEL-DRIVEN TRANSFER LEARNING

Wei Zhang[1], Zhipeng Li[1], Yiduo Guo[1], Ao Qiu[1,2], Yanjun Li[1], and Yibing Shi[1]*

[1]School of Automation Engineering, University of Electronic Science and Technology of China
[2]Welltech Research and Design Institute of China Oilfield Services Co.
Emails: weizhang@uestc.edu.cn, lizhipeng1202@std.uestc.edu.cn, yiduoguo@163.com, qiuao@cosl.com.cn , yjli@uestc.edu.cn, ybshi@uestc.edu.cn

ABSTRACT

Time-of-flight (ToF) of ultrasonic waves is essential for petroleum well logging to draw borehole-wall images. This paper proposed a method that boosted accuracy of ToFs estimation in a complex geological environment. Unlike other classical methods, the proposed one adopts a one-dimensional convolutional neural network (1D-CNN) as a backbone to extract latent information related to ToF. For handling the shortage of ultrasonic waves with annotated ToFs, theoretical ultrasonic waves generated by manifold mathematical models are utilized as source domain to train the model, which is applied to estimate practical ultrasonic ToFs. Furthermore, since the distribution divergences exist between theoretical ultrasonic models and practical ones, Maximum Mean Discrepancy (MMD) and CORrelation ALignment (CORAL) as discrepancy loss functions are used to evaluate the distribution divergences between two domain datasets and to optimize the entire model. Tests on the ultrasonic waves acquired by an experimental well logging device demonstrate the proposed method has satisfactory performances.

Index Terms— ultrasonic imaging well logging, time-of-flight, transfer learning, MMD, CORAL

1. INTRODUCTION

Ultrasound is a significant type of mechanical wave that can propagate effectively in gas, liquid, solid or solid melt, and record information about different media [1]. In the Oil-Gas exploration, according to different measuring principle, sonic logging technologies are divided into long-spaced sonic logging [2], cross-dipole array acoustic logging [3], ultrasonic imaging logging (UIL) [4]. Compared with the previous two logging methods, ultrasonic image logging can provide intuitive insights on reservoir stratum by drawing borehole wall images, which has attracted enormous attention. Fig.1 illustrates the principle of depicting borehole walls while being in the reflection mode. As shown in Fig.1, ultrasonic waves after emitted could be reflected and refracted when striking borehole walls due to different acoustic impedance. Successively measuring the interval between transmitting pulse signals and receiving corresponding ultrasonic echo around the borehole, images of the borehole diameter can be achieved at a certain depth. Meanwhile, the image of the entire borehole wall will be drawn by moving the well logging instrument in the vertical direction [5]. Accordingly, imaging quality depends on whether accurately detecting the intervals between pulse excitation and receiving ultrasonic waves, i.e., Time-of-Flight (ToF) [6].

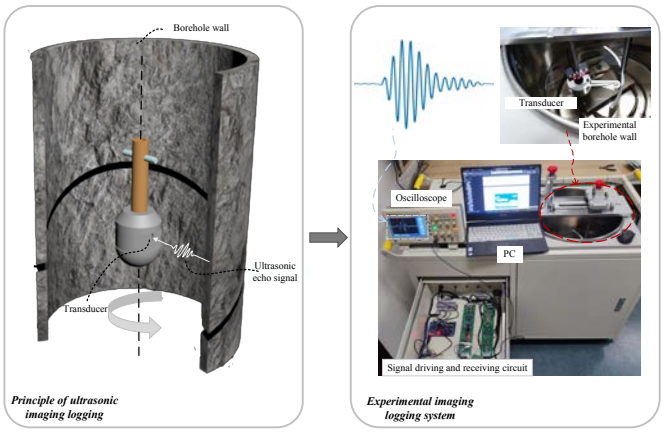

Fig. 1: From left to right: The principle of ultrasonic imaging logging; Experimental device for collecting actual signals. Our task is to research a transfer learning method for ToFs estimation from theoretical ultrasonic signals to real ones.

This paper focuses on how to improve ToFs estimation when the ultrasonic imaging logging tool operates in the oil-based mud, which can be regarded as a digital ultrasonic signal processing issue [7]. For the digital instrument, discrete signal processing algorithms were proposed successively, which included the Short-term average/Long-term average (STA/LTA) distinguishing changes of signals [8], Akaike In-

* represents corresponding author. This work was supported by China National Offshore Oil Corporation under Grant CNOOC-KJ ZDHXJSGG YF 2019-02.

formation Criterion (AIC) using higher- order statistics [9], Teager Kaiser energy operator (TKEO) based on energy spectrum analysis [10]. However, these methods rely on filters pre-processing echo signals before conducting ToFs estimation. And they merely estimate ToFs according to a single prior characteristic, which tends to produce a large deviation if ultrasonic echos are merged by other unknown signals. On the other hand, from diverse theoretical or empirical perspectives, continuous ultrasonic waves sensors receiving were modeled as superimposed Gaussian echoes with noise [11], damped sinusoid echos [12], or double exponential echos [13]. Based on ultrasonic mathematical models, combined with experimental data, researchers attempted to fit actual ultrasonic signals in order to perform ultrasonic parameters estimation such as ToFs, amplitude, or frequency in certain scenarios [14]. The accuracy of ToFs estimation depends upon whether the distribution of modeled signals matches real ultrasonic waves. Generally, a single model was selected as a foundation to deduce a special model, which indicates it cannot fit multiple types of ultrasonic signals. With the deep neural network (DNN) technique developing, it is possible to learn a multi-distribution model to deal with different tasks in complex environments [15], which employ different feature extractors such as convolutional neural networks (CNN) and its improved architectures [16].

In this paper, the model-driven transfer learning network (MDTLN) is built to learn a multi-distribution model from mentioned three representative models to implement ToFs estimation in ultrasonic imaging logging. Based on the transfer learning method, we construct a joint DNN model to bridge the gap in high dimensional space between ultrasonic mathematical models and real signals. Results show this strategy is able to carry out more accurate ToFs estimation in practice.

2. DETAILED METHODS

As mentioned previously, to deal with the shortage of ultrasonic signals with labeled ToFs, MDTLN utilizes a transfer learning strategy consisting of the CNN-based framework and distribution alignment method. The proposed method aims at learning latent feature distribution in several theoretical ultrasonic models and adapting parameters for the collected practical echos. The entire framework of MDTLN is illustrated in detail in Fig.2.

Specifically, we define $\mathcal{X}$ as input space, and $\mathcal{Y}$ as output space. Source domain is defined as $\mathcal{D}_s = \{\boldsymbol{x}_i, y_i\}_{i=1}^{N_s}$, in which $\boldsymbol{x_i} = \left[x_i^{(1)}, x_i^{(2)}, x_i^{(3)}, ..., x_i^{(n)}\right] \in \mathcal{X}$ denotes input ultrasonic signals generated by mathematical models, $y_i \in \mathcal{Y}$ denotes the corresponding labeled ToF. Data on the source domain is used to train the network model with weights. Meanwhile, target domain can be defined as $\mathcal{D}_t = \left\{\boldsymbol{x}_j, y_j^{(?)}\right\}_{j=1}^{N_t}$ without labeled annotations, where $\boldsymbol{x}_j = \left[x_j^{(1)}, x_j^{(2)}, x_j^{(3)}, ..., x_j^{(n)}\right] \in \mathcal{X}$ is the practical echo signal without ToF, and $y_j^{(?)}$ represents unknown ToFs on the target domain. Due to divergence of data between source and target domain, the joint probability distribution on the source domain $P_s(\boldsymbol{x}, y)$ is different from the corresponding one on the target domain $P_t(\boldsymbol{x}, y)$, i.e., $P_s(\boldsymbol{x}, y) \neq P_t(\boldsymbol{x}, y)$. Therefore, taking advantage of source data, our task is to seek a prediction function $f : \boldsymbol{x}_t \longmapsto y_t$ on the target domain, which makes f produce the minimum prediction errors ϵ of ToFs on the target domain, i.e., $f = arg\min E_{(\boldsymbol{x},y)\in\mathcal{D}_t}\left[\epsilon\left(f\left(x\right), y\right)\right]$.

As shown in Fig.2, the framework of MDTLN comprises a one-dimensional convolutional neural network (1D-CNN) and fully-connected neural network (FC-NN). 1D-CNN, which is adopted as the feature extractor, is built on four blocks where there are convolutional layers, an activation layer employing ReLU function, and a downsampling layer, respectively. The output channels of each block are 64, 128, 256, and 512 in sequence. Following the 1D-CNN blocks, the FC-NN block includes two fully-connected layers (FCL) and an output layer that generates the sampling point corresponding to the ToF. Different from the traditional regression problem based on DNN, given the distribution discrepancy of data between two domains, the trained model on the source domain tends to overfit the ToFs of the actual ultrasonic echos on the target domain if applied directly. Consequently, considering the structural risk minimization, the final optimization objective of MDTLN should be formulated as

$$f^* = \underset{f\in\mathcal{H}}{arg\min}\frac{1}{N_s}\sum_{i=1}^{N_s}\ell\left(f\left(\boldsymbol{x}_i\right), y_i\right) + \lambda D\left(\mathcal{D}_s, \mathcal{D}_t\right), \quad (1)$$

where $\mathcal{H}$ denotes hypothetical space, ℓ is the loss function, $D(\cdot,\cdot)$ stands for transfer regularization where we use the explicit distribution difference metric in this paper, and λ is a regularization parameter controlling the impact of regularization term on the proposed model.

In a training iteration, first, we forward source ultrasonic echo signals into MDTLN to gain the estimated value, which is used to calculate loss value with its corresponding labeled ToF, in which the mean squared error (MSE) for regression analysis is to evaluate the differences between the model's output values and labels. Second, the weights of the network are fixed, and source and target ultrasonic signals are simultaneously forwarded into MDTLN to calculate feature distribution discrepancy, which is employed to adjust the weights of MDTLN. In the designed architecture, we select the output of the first fully-connected layer (FC-1) as the basis for the evaluation of feature differences, and the maximum mean discrepancy (MMD) [17], and CORrelation ALignment (CORAL) [18] are introduced to calculate the feature discrepancy be-

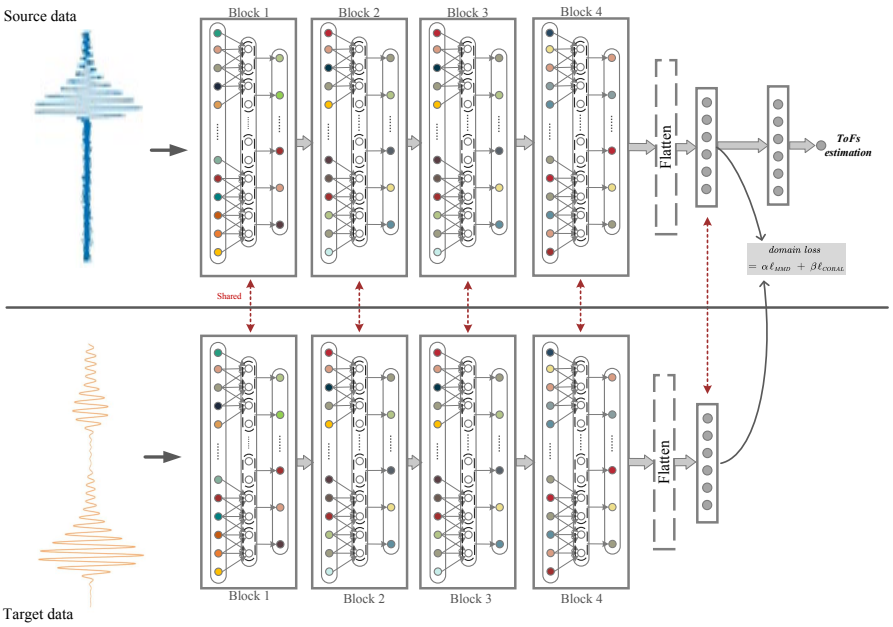

Fig. 2: The architecture of MDTLN.

tween two domains jointly. MMD is expressed as

$$\ell_{mmd}\left(\boldsymbol{X_s}, \boldsymbol{X_t}\right) = \left\| \frac{1}{n_s} \sum_{\boldsymbol{x_i} \in \boldsymbol{X_s}} \phi\left(\boldsymbol{x_i}\right) - \frac{1}{n_t} \sum_{\boldsymbol{x}_j \in \boldsymbol{X}_t} \phi\left(\boldsymbol{x}_j\right) \right\|, \tag{2}$$

where $\phi(\cdot)$ is the mapping function as which the proposed network uses the representation of FC-1 output. CORAL loss as the distance between covariances of the source and target features is formulated as

$$\ell_{CORAL} = \frac{1}{4d^2} \left\| C_S\left(\phi\left(x_i\right)\right) - C_T\left(\phi\left(x_j\right)\right) \right\|_F^2 \tag{3}$$

where $\|\cdot\|_F^2$ denotes the squared matrix Frobenius norm. C_S and C_T are respectively given by

$$C_S = \frac{1}{n_s}\left({D_S}^{\mathrm{T}} D_S - \frac{1}{n_s}\left(\boldsymbol{e}^{\mathrm{T}} D_S\right)^{\mathrm{T}}\left(\boldsymbol{e}^{\mathrm{T}} D_S\right)\right), \tag{4}$$

$$C_T = \frac{1}{n_T}\left({D_T}^{\mathrm{T}} D_T - \frac{1}{n_T}\left(\boldsymbol{e}^{\mathrm{T}} D_T\right)^{\mathrm{T}}\left(\boldsymbol{e}^{\mathrm{T}} D_T\right)\right), \tag{5}$$

where $\boldsymbol{e}$ represents a column vector in which all elements are 1. $D_S\left(D_T\right)$ denote the feature vectors. Accordingly, the final optimization objective can be written as

$$f^* = arg\min_{f \in \mathcal{H}} \frac{1}{N_s} \sum_{i=1}^{N_s} \ell\left(f\left(\boldsymbol{x}_i\right), y_i\right) + \alpha \ell_{mmd} + \beta \ell_{CORAL}. \tag{6}$$

Algorithm 1 summarizes the proposed model.

Algorithm 1 MDTLN

Input: preset parameters, $\mathcal{D}_s$, $\mathcal{D}_t$
Output: weights of the model after feature alignment

while epoch does not reach the default **do**
  for each batch in $\mathcal{D}_s$ **do**
    forward $\boldsymbol{x_i}$ into the network
    obtain FC-1 output
    calculate the MSE loss with labels
  end for
  keep weights of network constant
  for each batch in $\mathcal{D}_t$ **do**
    forward $\boldsymbol{x_j}$ into the network
    obtain FC-1 output
  end for
  calculate MMD and CORAL loss
  update weights of the network using Equation (6)
end while

3. EXPERIMENTS AND RESULTS

3.1. Experiment setup

As shown in the right part of Fig.1, we develop an experimental imaging logging system to provide practical ultrasonic waves, which is employed as target data to verify our proposed method. The central frequency of target ultrasonic is 250KHz which is sampled at a sampling frequency of 20MHz. In the source domain, total 10,000 sets of theoretical ultrasonic models as source domain with different ToF labels are employed to train the model. Meanwhile, total 58 sets

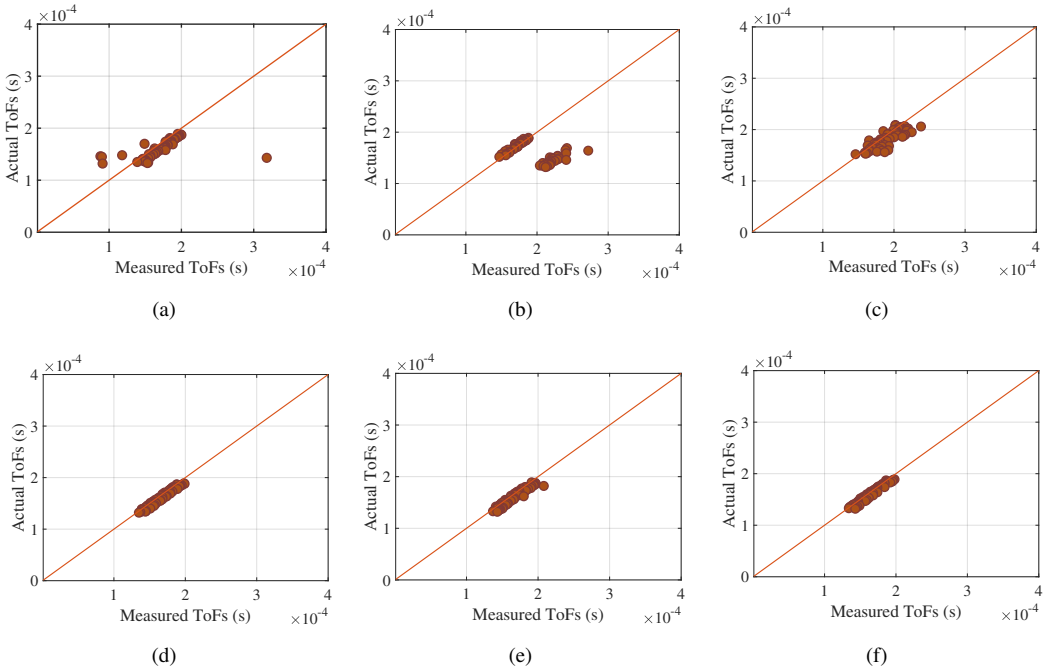

Fig. 3: Results of ToFs estimation via different algorithms. From (a) to (f): STA/LTA; AIC; TKEO; MDTLN based on MMD only; MDTLN based on CORAL only; MDTLN based on MMD and CORAL.

Table 1: Performances comparison of different approaches.

Approaches	**RMSE** (s)	**R-Square**
STA/LTA	4.18×10^{-5}	0.029
AIC	4.98×10^{-5}	-1.911
TKEO	1.38×10^{-5}	0.568
MDTLN (MMD only)	6.70×10^{-6}	0.855
MDTLN (CORAL only)	7.82×10^{-6}	0.798
MDTLN (MMD + CORAL)	$\mathbf{5.08 \times 10^{-6}}$	**0.904**

of ultrasonic waves where ToFs are determined manually are prepared for testing. The hyperparameters of MDTLN for training are set as following: epoch is 100, the initial learning rate is 1×10^{-7} which is decreased down to 0.8 times of the last one after every ten epochs, optimizer is stochastic gradient descent (SGD). The entire network is trained and tested on a hardware platform equipped with R5 2600 CPU@3.7GHz with 32G RAM and RTX 2060 GPU with 6G RAM.

3.2. Results

Fig.3 visualizes the testing results of ToFs estimation by previous algorithms and different schemes of feature discrepancy evaluation. The orange line termed the trend line on the diagram denotes measured ToFs equaling to actual ones, and the brown dots are the distributions between measured ToFs and corresponding actual ToFs. Obviously, the results generated by MDTLN, which are shown in Fig.3 (d), (e), and (f), are closer to the trend line than the other approaches. These visual results diagram that the deviations between the actual ToFs and the measured ones are relatively small using the proposed approach.

Table.1 gives the quantitative results of different approaches. Root Mean Squared Error (RMSE) and R square (R^2) are applied to evaluate the accuracy of different approaches. Compared with three classical methods, RMSEs gained through the trained MDTLN can be within $7\mu s$, and R^2 is increased up to 0.8, which means the proposed method can greatly improve the accuracy of ultrasonic ToFs. On the other hand, the proposed network optimized by MMD and CORAL loss jointly can bridge the gap between source and target domain further, which has a positive impact on the accuracy of ToFs estimation.

4. CONCLUSIONS

In this paper, we conduct research on ultrasonic ToFs estimation in the well logging tool. The MDTLN based on transfer learning is proposed, which adopts the theoretical mathematical ultrasonic models as source data to train the model, and transfers the learned one into ToFs estimation of actual ultrasonic signals by joint feature discrepancy alleviation. Tests on the experimental logging systems prove the feasibility of model migration on the ToFs estimation of ultrasonic waves.

5. REFERENCES

[1] H. Yamawaki and T. Saito, "Numerical calculation of ultrasonic propagation with anisotropy," *NDT & E International*, vol. 33, no. 7, pp. 489–497, 2000.

[2] Aristotelis Dasios, Clive McCann, and Timothy Astin, "Least-squares inversion of in-situ sonic q measurements: Stability and resolution," *Geophysics*, vol. 69, no. 2, pp. 378–385, 2004.

[3] Junqiang Lu, Xiaodong Ju, and Xiangyang Cheng, "Design of a cross-dipole array acoustic logging tool," *Petroleum Science*, vol. 5, no. 2, pp. 105–109, 2008.

[4] Jie Zhang, Xin Nie, Suyun Xiao, Chong Zhang, Chaomo Zhang, and Zhansong Zhang, "Generating porosity spectrum of carbonate reservoirs using ultrasonic imaging log," *Acta Geophysica*, vol. 66, no. 2, pp. 191–201, 2018.

[5] Hongqi Liu, *Principles and Applications of Well Logging*, pp. 59–114, Springer Berlin Heidelberg, Berlin, Heidelberg, 2017.

[6] Patrick McVittie and Les Atlas, "Air-coupled ultrasound time-of-flight estimation for shipping container cargo verification," in *2008 IEEE International Conference on Acoustics, Speech and Signal Processing (ICASSP)*, 2008, pp. 1797–1800.

[7] Ladislav Jerabek, Anthony L. Bartos, and Jan Strycek, "Industrial application of acousto-ultrasonic signal quality and robust time-of-flight estimation for anisotropic materials," in *2011 IEEE International Conference on Acoustics, Speech and Signal Processing (ICASSP)*, 2011, pp. 1793–1796.

[8] Einar Agletdinov, Dmitry Merson, and Alexei Vinogradov, "A new method of low amplitude signal detection and its application in acoustic emission," *Applied Sciences*, vol. 10, no. 1, pp. 73, 2019.

[9] Yong Bao and Jiabin Jia, "Improved time-of-flight estimation method for acoustic tomography system," *IEEE Transactions on Instrumentation and Measurement*, vol. 69, no. 4, pp. 974–984, 2020.

[10] W. Yang, W. Luo, and Y. Zhang, "Automatic detection method for monitoring odontocete echolocation clicks," *Electronics Letters*, vol. 53, no. 6, pp. 367–368, 2017.

[11] R. Demirli and J. Saniie, "Model-based estimation of ultrasonic echoes. part i: Analysis and algorithms," *IEEE Transactions on Ultrasonics, Ferroelectrics, and Frequency Control*, vol. 48, no. 3, pp. 787–802, 2001.

[12] M. Parrilla, J.J. Anaya, and C. Fritsch, "Digital signal processing techniques for high accuracy ultrasonic range measurements," *IEEE Transactions on Instrumentation and Measurement*, vol. 40, no. 4, pp. 759–763, 1991.

[13] Guo Gang, Wang Shu-xun, Zhao Xiao-hui, and Sun Xiao-ying, "Double exponential model of ultrasonic signals," in *2008 9th International Conference on Signal Processing*, 2008, pp. 2575–2578.

[14] Wen-Jiao Zhu, Ke-Jun Xu, Min Fang, Wei Wang, and Zi-Wen Shen, "Mathematical modeling of ultrasonic gas flow meter based on experimental data in three steps," *IEEE Transactions on Instrumentation and Measurement*, vol. 65, no. 8, pp. 1726–1738, 2016.

[15] Xuelian Ou, Guangrui Wen, Xin Huang, Yu Su, Xuefeng Chen, and Hailong Lin, "A deep sequence multi-distribution adversarial model for bearing abnormal condition detection," *Measurement*, vol. 182, pp. 109529, 2021.

[16] Nan Ren, Zaiming Fu, Dandan Zhou, Hanglin Liu, Zhong Wu, and Shulin Tian, "Jitter decomposition by convolutional neural networks," *IEEE Transactions on Electromagnetic Compatibility*, vol. 63, no. 5, pp. 1550–1561, 2021.

[17] Yongchun Zhu, Fuzhen Zhuang, Jindong Wang, Jingwu Chen, Zhiping Shi, Wenjuan Wu, and Qing He, "Multi-representation adaptation network for cross-domain image classification," *Neural Networks*, vol. 119, pp. 214–221, 2019.

[18] Baochen Sun and Kate Saenko, "Deep coral: Correlation alignment for deep domain adaptation," in *European conference on computer vision*. Springer, 2016, pp. 443–450.